ACS ES&T Water

pubs.acs.org/estwater

Article

Analysis of Groundwater Flows under the Fukushima Daiichi Nuclear Power Plant Reactors Using Contaminated Water from 42 Subdrain Pits

Tamao Tanji, Makoto Furukawa, Seiji Taguma, Katsushige Fujimoto, Hikaru Sato, Naoaki Shibasaki, and Yoshitaka Takagai*

Cite This: *ACS EST Water* 2023, 3, 139−146

Read Online

ABSTRACT: We analyzed groundwater collected from 42 subdrain pits (wells) located around the reactor buildings of plant units #1 to #4 of the Tokyo Electric Power Company Fukushima Daiichi Nuclear Power Plant (F1-NPP) to understand the groundwater dynamics and water flows around F1-NPP. Since water samples collected from this small area exhibit very similar water quality, there are difficulties in understanding the flow dynamics of the groundwater using conventional chemical analyses. In this study, we clarified the groundwater flows using an altitude-modified principal component analysis (PCA) with a total of 798 data items (19 factors × 42 pits) in the chemical analyses. The PCA results showed that six specific pits deviated from the common values and that the others contained contributions from both the natural elements and radioactive nuclides. The groundwater flows under units #1−#4 into two flow lines originating from two main water sources were classified, and these lines merged around the bayside of unit #2 due to the lower groundwater head. This method proved suitable for elucidating the groundwater dynamics and water flows in this small area by the proposed altitude-modified PCA.

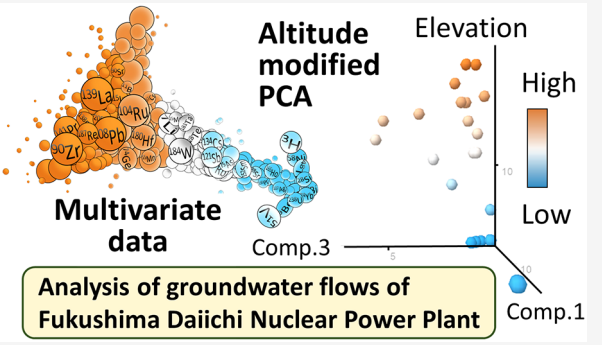

KEYWORDS: *groundwater analysis, multichemical components, principal component analysis, Fukushima Daiichi Nuclear Power Plant*

INTRODUCTION

Understanding groundwater dynamics and water flows is very important for predicting future issues related to contamination of water so that suitable measures can be implemented in advance and/or for taking effective actions in advance to alleviate undesired future issues like discharging contaminated water into the ocean. However, it is not easy to understand the groundwater dynamics and flows in a small area because of the small differences in the chemical species and their concentrations (i.e., the water quality) obtained using conventional chemical analyses.

The Tokyo Electric Power Company (TEPCO) Fukushima Daiichi Nuclear Power Plant (F1-NPP) were damaged in 2011, and the area of the site covers only 3.5 square km. There are 42 subdrain pits (wells) around reactor buildings of units #1−#4. The role of the pits is to control water levels, and sampling from the pits and monitoring of the radioactivity concentration have been conducted regularly since the accident.[1,2] Oddly enough, the hotspots that contain contaminated water (in the subdrain pits) are scattered all over the site, and it has been difficult to find any continuities or relationships between the contaminated locations and the groundwater flows from the results of the radioactivity analyses. So far, hydrological research has been performed only for groundwater flows that span large areas around the F1-NPP like a unit of stratum across counties[3] or neighboring prefectures;[4] however, the analytical data from the subdrain pits in the site have never been connected to their radioactivity. If characteristic constituents, such as molybdenum,[5] arsenic,[6] and high concentrations of silicates,[7] are eluted into the groundwater and if the distribution of the concentration gradients of these ions can be detected, analyses of the flows or dynamics would be relatively understandable. However, since the chemical properties of even stable isotopes are very similar in such a small area, it is difficult to find the differences. Although many researchers are aware of the importance of such discrimination, understanding the dynamics of groundwater flows for a small area remains challenging.

Received: September 15, 2022
Revised: November 19, 2022
Accepted: November 21, 2022
Published: December 8, 2022

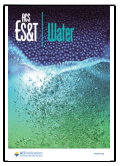

To classify water quality, researchers commonly use a hexa-diagram method. In this method, the ion equivalents for six or seven typical chemical species are plotted as a hexa-diagram (as shown in Figure 1). The water quality can then be recognized visually from the shape of the diagram, which depends on the concentrations of the typical species.[8]

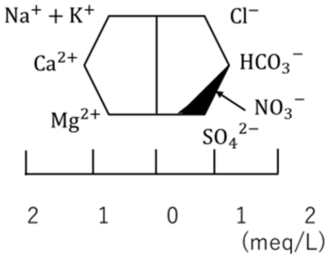

Figure 1. Typical hexa-diagram characterization method for environmental water.

While a hexa-diagram is advantageous when there are great differences in its shape (i.e., for the case with typical differences in water quality), it is not easy to detect differences in the shape of the diagram visually for water samples collected from very closely spaced locations that have almost the same water quality. Even if we add more variables to the diagram, this difficulty in discrimination basically does not change. Thus, the conventional hexa-diagram method is fundamentally not able to elucidate the analysis of water dynamics or the flows in a small area, even when many data from various chemical analyses are provided.

Principal component analysis (PCA)[9] is a typical method for multivariate analyses, and it is used in combination with chemical analyses in many fields, including authenticity determination,[10] origin determination,[11] and bioinformatics.[12] While a plethora of reports have been published concerning the combination of PCA and chemical analyses, most applications to inorganic analysis commonly use quantitative data for a few elements focusing on the target (e.g., some pollutants or their isotope ratios in the natural elements are mainly used).[13] This differs from bioinformatics, in which there are certain regularities in the pairings—such as amino acid or base sequences in DNA—that make it easy to apply to informatic analysis. In contrast, there is no literature concerning applications to the analysis of groundwater dynamics using large amounts of data that contain many chemical components from many sampling locations; consequently, the abovementioned hexa-diagram method has been commonly used as a traditional method. The PCA can reduce many variables into a smaller number of derived variables that may be readily visualized in two- or three-dimensional space.

In this study, we measured the concentrations of 15 isotopes and 3 anthropogenic radionuclides and Gross β radioactivity in groundwater samples obtained from 42 subdrain pits around reactor buildings of units #1−#4 of F1-NPP during 2016 using inductively coupled plasma mass spectrometry (ICP-MS) and radioactivity analysis. We analyzed the resulting 798 data items using both a normal PCA and a modified PCA that incorporated elevations. We used this approach to clarify the groundwater dynamics and flows under the F1-NPPs, which are all located in a small area.

EXPERIMENTAL SECTION

Apparatus. NexION 300S ICP-MS (PerkinElmer, Inc., Shelton, CT) equipped with a dynamic reaction cell (DRC) and a quartz baffled cyclonic spray chamber with a concentric nebulizer was used. We employed ultrapure argon (Ar) gas (>99.999%) for the Ar plasma and helium (He) gas (>99.999%) as the collision/reaction gas to remove mass spectral interference. The kinetic energy discrimination (KED)[14] mode in the DRC was employed, and the resultant concentrations were obtained without the influence of interference.

Reagents and Preparation. We prepared mixture solutions of 15 elements by mixing Multielement Calibration Standard series #2, #3, #4, and #5 as the standard stock solutions for the metal-ion mixtures (stable isotopes with concentrations of 10 mg/L; PerkinElmer). We also used ultrapure concentrated HNO_3 (ultrapure-grade, 61 w/w %; Kanto Chemical Co., Inc., Tokyo, Japan) and perfluoroalkoxy alkane (PFA) bottles and containers (AS-ONE Co. Tokyo Japan). We obtained ultrapure water (18.2 MΩ·cm) from a PURELAB Ultra purifier (ELGA, Bucks, U.K.).

Sampling and Sample Preparation. Groundwater samples collected from 42 subdrain pits around reactor buildings of units #1−#4 of F1-NPP during 2016 were used. The samples were stored at temperatures below 4 °C. We performed the sample treatments and measurements in a hot lab inside F1-NPP.

Figure 2A shows a map with the geomorphological locations. The sampling locations are shown as a map of the wells in Figure 2B. In addition, Table S1 in the Supporting Information provides other information about the samples, such as the sampling date, type of well,[15] and grid data. There are three types of subdrain pits in F1-NPP. One is a normal type of single well; the second also is a normal type, but it is connected to neighboring wells; and the third is much deeper than a normal type of single well.

The concentrations of radioactive ^3H, ^{134}Cs, ^{137}Cs, and Gross β were measured by TEPCO, and we measured the same samples again using the ICP-MS method to quantify the isotopes. Table 1 shows the input data for ^3H, ^{134}Cs, ^{137}Cs, and Gross β radioactivity, which were provided by TEPCO. [Note: Based on legal regulations, the numerical data for the radioactivity concentrations were publicly press-released in advance via the TEPCO website.[2] For the Gross β radioactivity, the radioactivity might be influenced by the detection efficiency of individual radionuclides (e.g., energy region). Hirayama previously reported the analysis of Gross β values in the methods of TEPCO from the viewpoints of the dependence for radionuclides to get a detector response, and the actual activity of ^{134}Cs contributed 66% values to the values of Gross β.[16]] We converted the radioactivity concentration (Bq L^{-1}) to mass concentration (g L^{-1}) using eq 1

$$C = \left(A\frac{t_{1/2}M}{\ln 2N_A}\right)/V \quad (1)$$

where C is the mass concentration of the target nuclide (g L^{-1}), A is the radioactivity (Bq), $t_{1/2}$ is the half-life of the nuclide (s), M is the mass number of the target nuclide, N_A is Avogadro's number, and V is the sample volume (L).

In addition, Gross β is pure β-particle emission, which might be contributed from mainly ^{134}Cs, ^{137}Cs, ^{90}Sr ($t_{1/2}$ = 28.8 y), and its daughter nuclide ^{90}Y ($t_{1/2}$ = 64 h, 100% β-emitter).[17]

https://doi.org/10.1021/acsestwater.2c00455
ACS EST Water 2023, 3, 139−146

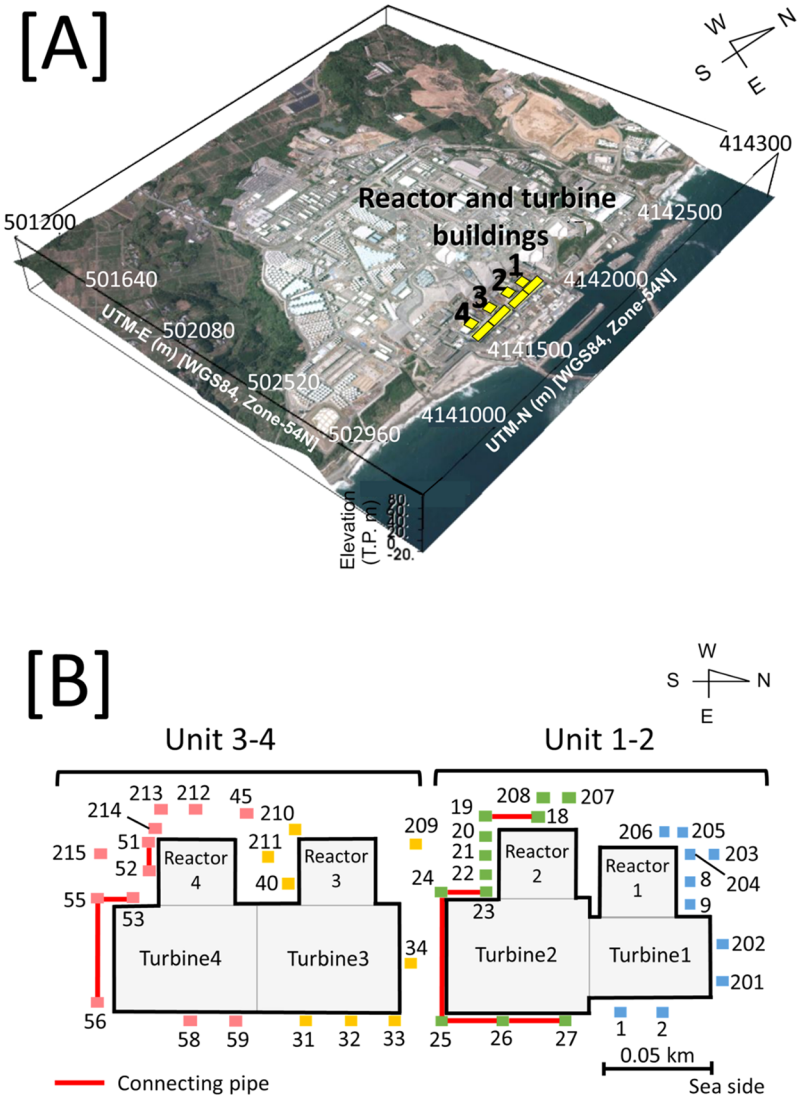

Figure 2. Map and overview of the Fukushima Daiichi Nuclear Power Plant (F1-NPP). [A] Overview of F1-NPP showing its geomorphological setting. The aerial photograph provided by the Geospatial Information Authority of Japan (GSI). [B] Locations of the subdrain pits (wells). The assigned pit numbers correspond to those given in the official announcement reported by the Japanese government and TEPCO.[18] The blue, green, yellow, and red dots represent the pits belonging to reactor buildings of units #1, 2, 3, and 4, respectively. The red lines are horizontal pipes connected to each pit.

[Note: U and Th did not impact on PCA due to their lower concentration and even inclusion in all samples.]

Data Analysis. For the data analysis, the information of concentrations of alkali metal elements, alkaline earth metal elements, and the elements up to the third period in the periodic table (Li, Be, B, Mg, Ti, Cr, Mn, Ni, Cu, Ga, As, Rb, Sr, Cs, Ba) was obtained using ICP-MS, and the factors were selected from reliable data, which shows that the concentrations were certainly quantified using calibration curves with good linearity of the correlation coefficient of 0.975 or higher and using values over the limits of detection (LODs). The data of the anthropogenic radionuclides (^{3}H, ^{134}Cs, ^{137}Cs) and Gross β radioactivity in the sample water collected from subdrain pits presented by TEPCO were used. We thus inputted 19 factors to the PCA as the dataset (15 isotopes and 3 anthropogenic radionuclides and Gross β radioactivity) obtained from each of 42 sampling points; i.e., 798 data items.

We performed the PCA using the computer software analytics platform TIBCO Spotfire (Palo Alto, CA). For the data analysis, we standardized the mean and the variance of the quantitative values for each isotope as 0 and 1, respectively.

RESULTS AND DISCUSSION

Simultaneous Multielement Quantification. Table S2 in the Supporting Information shows the concentrations of 15 elements measured using ICP-MS in the contaminated water from 42 subdrain pits. To perform this quantification, we used calibration curves with correlation coefficients of at least 0.975. This table also shows the LOD for each element. To avoid MS spectral interference, we employed the KED mode using He gas.[14] The interferences were not confirmed in the quantification. In the PCA, we did not use any of the data for those elements with concentrations below their respective LODs.

Principal Component Analysis (PCA). Table 2 shows the PCA loading values for 19 factors from 42 sampling points. The contributions from the 1st, 2nd, and 3rd principal

https://doi.org/10.1021/acsestwater.2c00455
ACS EST Water 2023, 3, 139−146

Table 1. Input Data of the Concentration of Anthropogenic Radionuclides and Gross β Radioactivity[1,3]

subdrain pit # [2]	radioactivity/Bq L^{-1}			
	^{3}H	^{134}Cs	^{137}Cs	gross β
1	26,000	11	75	83
2	11,000	<LOD(3.6)	4.3	<LOD(11)
8	<LOD(120)	14	83	82
9	770	<LOD(4.3)	18	20
18	290	190	1200	1400
19	510	130	850	970
20	740	<LOD(5.6)	<LOD(4.4)	17
21	<LOD(110)	<LOD(4.8)	14	14
22	190	6.6	44	36
23	160	77	460	1100
24	240	45	270	350
25	130	61	400	600
26	<LOD(120)	11	88	130
27	<LOD(110)	21	150	250
31	<LOD(120)	12	92	250
32	<LOD(110)	<LOD(5.9)	<LOD(6.4)	<LOD(12)
33	<LOD(120)	7.0	27	44
34	170	27	180	190
40	270	210	1300	1500
45	<LOD(100)	<LOD(4.1)	<LOD(4.3)	<LOD(12)
51	<LOD(100)	<LOD(3.5)	<LOD(5.0)	<LOD(12)
52	<LOD(130)	<LOD(8.9)	<LOD(15)	<LOD(18)
53	<LOD(130)	<LOD(9.3)	<LOD(18)	<LOD(11)
55	<LOD(130)	<LOD(10.0)	<LOD(16)	<LOD(11)
56	150	<LOD(4.1)	<LOD(5.2)	<LOD(10)
58	<LOD(130)	<LOD(10.0)	18	<LOD(12)
59	150	<LOD(3.5)	6.7	<LOD(15)
201	<LOD(120)	<LOD(5.8)	<LOD(5.2)	<LOD(10)
202	<LOD(120)	<LOD(4.6)	<LOD(4.4)	<LOD(10)
203	<LOD(120)	<LOD(5.6)	<LOD(5.6)	<LOD(10)
204	<LOD(120)	<LOD(4.3)	5.9	21
205	<LOD(120)	<LOD(4.7)	<LOD(3.8)	<LOD(10)
206	<LOD(110)	<LOD(6.9)	15	20
207	<LOD(110)	<LOD(4.4)	<LOD(5.4)	17
208	<LOD(110)	<LOD(4.4)	<LOD(3.8)	<LOD(12)
209	<LOD(110)	<LOD(3.6)	<LOD(4.9)	<LOD(13)
210	<LOD(100)	<LOD(3.9)	3.6	<LOD(12)
211	<LOD(100)	<LOD(4.2)	16	54
212	<LOD(100)	<LOD(3.7)	<LOD(3.9)	<LOD(12)
213	<LOD(100)	<LOD(4.5)	<LOD(3.4)	12
214	400	<LOD(4.4)	8.0	15
215	<LOD(130)	<LOD(11)	<LOD(14)	<LOD(18)

[1]The data presented by the Tokyo Electronic Power Company Holding Ltd 2. [2]Identification numbers of the subdrain pits corresponding to the number on the map in Figure 2B. [3]<LOD: the value is less than the limit of detection (LOD). The values in parentheses are LOD.

components are listed as Comp. 1, Comp. 2, and Comp. 3, and they were 16.70, 13.77, and 12.59%, respectively. The increases of the radioactivity concentration contributed to the positive value of Comp. 1 and also the negative value of Comp. 2. The isotopes originated from the environment contributed to the negative way of Comp. 3. The cumulative contributions from these three principal components totaled 43.06%. In previous applications that used PCA to identify various organic substances for environmental analysis, cumulative contributions lower than 40% were reported.[19−21] These values (<40%) were reported even in wide-area investigations. Compared with these values, our value of 43.06% is entirely satisfactory for our small-area investigation.

Table 2. Loadings[a]

elements	loadings		
	comp. 1	comp. 2	comp. 3
^{137}Cs	0.21	−0.34	0.42
^{134}Cs	0.20	−0.34	0.41
^{63}Cu	0.14	−0.23	0.08
^{7}Li	0.13	0.39	0.23
^{11}B	0.12	−0.18	0.09
^{69}Ga	0.11	0.44	0.37
gross β	0.11	−0.20	0.24
^{25}Mg	0.10	−0.04	0.02
^{85}Rb	0.09	0.02	−0.04
^{138}Ba	0.09	0.45	0.37
^{48}Ti	0.07	−0.02	−0.24
^{75}As	0.02	0.09	−0.14
^{55}Mn	0.01	0.23	−0.17
^{88}Sr	−0.02	−0.14	−0.14
^{52}Cr	−0.04	−0.04	−0.10
^{9}Be	−0.13	−0.04	−0.01
^{58}Ni	−0.50	−0.05	0.19
^{133}Cs	−0.52	−0.04	0.20
^{3}H	−0.52	−0.04	0.20
contributing factor rate, %	16.70	13.77	12.59
cumulative contribution factor rates, %	16.70	30.47	43.06

[a]The loadings are shown in descending order of the first principal components.

Figure 3 shows a plot of the principal component scores for each subdrain pit. Since the subdrain pits are located adjacent to each reactor building, the plots are color-coded for each building. For 36 of the 42 subdrain pits, the main contribution to the PCA score came from Comp. 1. It is considered that Comp. 1 indicates the similarity of groundwater.

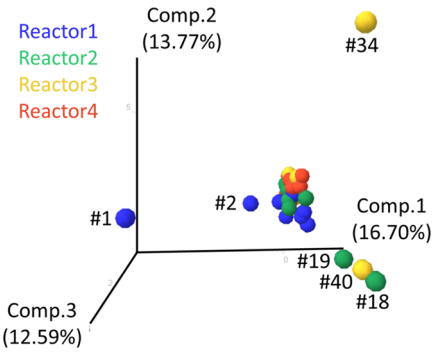

Figure 3. PCA score plot in subdrain waters of F1-NPP. The blue, green, yellow, and red colored points represent the subdrain pits around reactor buildings of units #1, #2, #3, and #4 (cf., the map in Figure 2B). [Attention] The plot size is not related to any factors. All plots are the same size; however, the different sizes of plots depending on the perspective may be seen.

For pits #1, #2, #18, #19, #34, and #40, the PCA score plots were obviously different from those of other samples. From these PCA results, pits #1, #2, #18, #19, #34, and #40 were plotted out of the main population mostly due to

https://doi.org/10.1021/acsestwater.2c00455
ACS EST Water 2023, 3, 139−146

anthropogenic radionuclides and Gross β radioactivity. Figure S2 in the Supporting Information shows the result of hierarchical cluster analysis; however, it was difficult to identify groundwater flows. The six pits (#1, #2, #18, #19, #34, and #40) were classified as the category of high radioactivity concentrations by the hierarchical cluster analysis; however, it was obvious before the PCA. At the F1-NPP site, three types of subdrain pits exist, as noted before; they are normal single wells, normal wells that are connected to neighbor wells, and deeper wells. The PCA scores show that there is no apprehension with these types of wells, as shown in Figure S3 in the Supporting Information. In addition, Figure S4 in the Supporting Information shows that the plotted points are roughly correlated with the reactor buildings (that is, by color), according to the scores of the first three principal components. Although the climate often impacts the quality of groundwater,[22,23] the sampling date did not influence the results of scores as shown in Figure S5 in the Supporting Information.

PCA Including Environmental Considerations. Although we identified specific elements that contributed to the PCA score, the connections between PCA and the continuity of fluid flows with each pit were not clear in that analysis (cf. Figure 4 and Table 2). However, the PCA approach was able to distinguish two regions between units #1 and 2 and units #3 and 4. This is reasonable because the reactor buildings and turbine buildings of unit #1 and unit #2 are architecturally connected buildings, and they are built on the same stratum. Similarly, units #3 and #4 are also architecturally connected buildings, and they are separated from the building containing units #1 and 2 (cf. Figure 2A). In addition, Figure S4 in the Supporting information shows the score plots that have similar trends between units 1 and 2 as well as between units 3 and 4. Meanwhile, the groundwater flows continuously in the higher (water level) to lower direction.[24] Based on this natural order, we recalculated the PCA results after adding a new absolute variable into the previous PCA. Figure 4 shows the modified plot of principal component scores after adding an axis for direction. There have been no reports to date concerning PCA that incorporates absolute values such as elevation as one of the axes of the PCA score plot. Figure 4A shows the connected building for units #1 and #2, and Figure 4B shows the connected building for units #3 and #4. The clusters of principal component scores capture the characteristics of the slight changes in each connected building. This confirms the tendency of water to flow continuously from a higher altitude (i.e., mountain side) to a lower altitude (i.e., sea side). Notably, two continuous flows are obviously confirmed. It is clear from the consideration of loading that the difference in water quality can be found in Comp. 3.

Figure 4C shows a map of the classification of groundwater flows specified by the PCA score values and altitude (using data from Figure 4A,B). We had expected a simple flow passing from the mountain side (west side) to the sea side (east side) and basically the simple flow was observed; however, contrary to our expectations, we actually found the following two different types of flows (as shown in Figure 4C). Namely, in the condition of the pits, which corresponded to the value of Comp. 3, the water-flow orders basically following the blue arrows were exhibited, which were formed based on the elevations, as shown in Figure 4A,B. Finally, the two flows are merged around pits [#25/#33]. There appear to be two main origins of groundwater flows from the mountain side to the

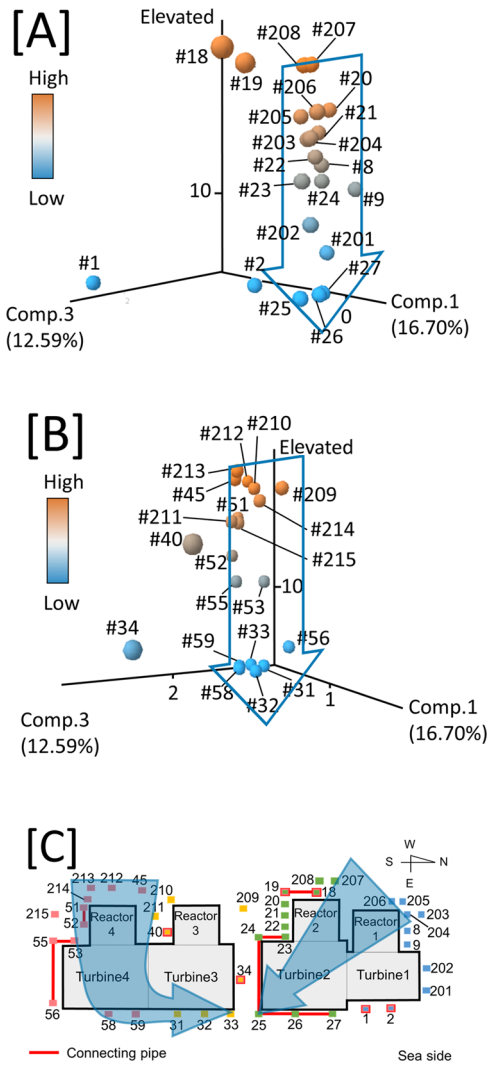

Figure 4. PCA score plots in subdrain waters collected around each building. [A] Connected buildings for units #1 and 2, [B] the connected buildings for units #3 and 4, and [C] groundwater flows presented by this study. The plotted colors correspond to grid data measured from the west side. See text for explanations of the flows indicated by the blue arrows. The red-border pits are determined to be stagnant from the results of PCA. [Attention] The plot size is not related to any factors. All plots are the same size; however, the different sizes of plots depending on the perspective may be seen.

reactors. Groundwater flows from the northwest (pits #203−#207) and the other flows from the west−southwest (pits #45 and #209−#213), and flows in the case of these latter pits are considered to have the same origin. It may be necessary to investigate the west side of the reactors to confirm this hypothesis; however, it has not been investigated in this study.

We also investigated pits #1, #2, #18, #19, #34, and #40, which were significantly different from other pits in the PCA. Pits #1 and #2 showed high concentrations of radioactivity and exhibited great differences not only from the properties of adjacent pits around units 1 and 2 but also from those of the other pits in the PCA classification. These results show that groundwater on pits #1 and #2 barely flows. Highly radioactive water samples contaminated by ^{3}H exist in pits #1 and #2; however, no impact on other pits was found (cf. Table S1 in the Supporting Information).

https://doi.org/10.1021/acsestwater.2c00455
ACS EST Water 2023, 3, 139−146

Although pits #207 and #208 were not almost contaminated by radioactive nuclides, we classified them with pits #18 and #19, which showed quite high concentrations of radioactive Cs. We consider that the groundwater from pits #207 and #208, which is supplied from the mountain side, merges with the highly contaminated water from pits #18 and #19. Therefore, pits #18 and #19 were affected more intensely by contamination from the reactor than from the minerals that originated from the groundwater. For pits #18, #19, #34, and #40, other PCA trials were conducted (i.e., substituting the values of the radioactivity concentration to other different values obtained from adjacent pits around unit building [#18 and #19 were for units 1 and 2; #34 and #40 were for units 3 and 4]). As a result, the waters of those pits were revealed as originating from the same source as other pits around each unit; however, the high concentration of the radionuclides was suggested to be stagnated into these pits by the results of the PCA score. Namely, a possibility is considered that groundwater is flowing into those pits but not flowing out from those pits.

Geological Validity. Among all 42 subdrain pits, the majority—38 pits—are 12−16 m deep. The other four pits are 40 m deep wells. Figure 5 shows cross sections around the F1-NPP together with the groundwater heads. In Figure 5, T.P. meters is the annual mean sea level values of Tokyo. Figure 5A shows a north−south cross section, with T.P. = 6.5, 5.0, 5.9, and 6.5 m for bottom of units #1, #2, #3, and #4, respectively.[25,26] The lowest level of T.P. is around unit #2. Figure 5B shows an east−west cross section (a slice containing unit #3). The groundwater head slopes drastically from the mountain side (west side) to the sea side (east side), and there is 450 m from unit #3 to the sea. These facts show that the groundwater basically flows from the mountain side (west side) to the sea side (east side). Since T.P. for unit #2 is lower than that for any of the other units (north−south), and the slope of the groundwater head is steeper (west−east), it is obvious that the groundwater gathers easily around unit #2. These hydrogeological considerations support the PCA results obtained in this study, which show that each groundwater flow congregates around pits #25/#33.

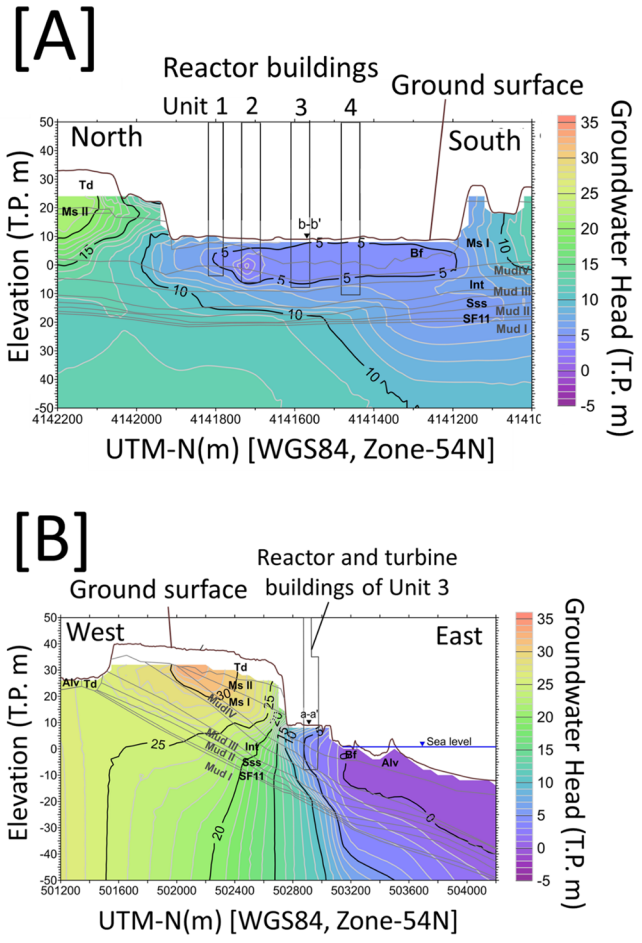

Figure 5. Cross sections of the simulated groundwater heads as of 11 March 2011.[30] [A] North−south and [B] west−east.

At the F1-NPP site, TEPCO built seaside impermeable walls (the wall is composed of 594 steel pipe sheet piles driven into the earth across a width of about 780 m) in October 2015 as a countermeasure to prevent the inflow of contaminated water from the surroundings into the sea.[27,28] For pits #58−59 (as shown in Figure 4C), the drastic change in the direction of the water flow is probably due to the blocking by this wall,[29] which changes the direction of migration of the water toward the lower groundwater head of unit #2.

CONCLUSIONS

In conclusion, it is difficult to specify groundwater flows that originate from the same stratum in a small area using the concentrations of various chemical components and water qualities (e.g., the use of a hexa-diagram). For F1-NPP, contaminated pits exist randomly, and the water quality due to the mineral content is very similar due to very close proximity of the sampling points. Consequently, the significance of continuous flows of groundwater and water dynamics was not previously recognized. This study successfully clarified the flows of groundwater below the small 3.5 square km site of F1-NPP using a modified PCA with a total of 798 data items (19 factors × 42 pits) obtained using ICP-MS and radioactivity analysis. The PCA showed that six specific pits were different from others. The score plots and their loadings led to the identification of contributing factors that originated from geology rather than from radioactive materials. We discussed these 6 pits individually. Contrary to our expectations, the PCA revealed two groundwater flows and two origins of the groundwater (from the northwest and from the west−southwest). We found that groundwater for those 6 pits (#1, #2, #18, #19, #34, and #40) is stagnant, and the active flows of each pit are analyzed. In addition, two major flows migrate in the direction of unit #2 (i.e., pits #25/#33). For flow units 3 and 4, the seaside impermeable wall built in October 2015 may prevent the flow of the contaminated water from leaking into the ocean; it changed the direction of water migration toward the direction of units #3−#4, which has a lower level of T.P. These results are consistent with the geological considerations.

In 2022, the concentrations of Gross β in seawater (at the bay entrance in front of units #1−#4) were about 10−30 Bq L^{-1} (LOD: 8.7 Bq L^{-1}).[31] This suggests that it may be difficult to prevent completely a large amount of groundwater that contains a small amount of radioactive nuclides such as ^{3}H from leaking into the ocean. At present (2022), the circumstances of F1-NPP regarding groundwater may be different from the results obtained in this study because of both the decommissioning of F1-NPP and a variety of countermeasures to prevent rainwater and groundwater from flowing into the buildings. However, it is important to know

https://doi.org/10.1021/acsestwater.2c00455
ACS EST Water 2023, 3, 139−146

the original underground flows at the site as an archival reference. In particular, this study has demonstrated the existence of groundwater flows using water samples collected from closely spaced sampling points. In addition, our results enable the visualization and estimation of the circumstances of groundwater. For environmental analyses, this method provides an effective means for the visual recognition of slight differences in chemical components at levels that are different to recognize by other methods. In addition, knowing the migration patterns of groundwater not only enables predictions of the migration of pollutants but also enables an understanding of the dynamic nature of such flows.

■ ASSOCIATED CONTENT

Supporting Information

The Supporting Information is available free of charge at https://pubs.acs.org/doi/10.1021/acsestwater.2c00455.

Information of sampling waters (Table S1); element concentrations of subdrain pits (Table S2); diagrams of the 32 factors for subdrain water (Figure S1); dendrogram of the hierarchical clustering for subdrain water (Figure S2); PCA score plot for subdrain waters (Figure S3); PCA score plot of subdrain waters in each building (Figure S4); and PCA score plot of subdrain waters for each sampling date (Figure S5) (PDF)

■ AUTHOR INFORMATION

Corresponding Author

Yoshitaka Takagai − *Faculty of Symbiotic Systems Science, Cluster of Science and Technology, Fukushima University, Fukushima 960-1296, Japan; Institute of Environmental Radioactivity, Fukushima University, Fukushima 960-1296, Japan;* orcid.org/0000-0002-7760-5636; Email: s015@ipc.fukushima-u.ac.jp

Authors

Tamao Tanji − *Faculty of Symbiotic Systems Science, Cluster of Science and Technology, Fukushima University, Fukushima 960-1296, Japan*

Makoto Furukawa − *Faculty of Symbiotic Systems Science, Cluster of Science and Technology, Fukushima University, Fukushima 960-1296, Japan; PerkinElmer Japan Co., Ltd., Yokohama, Kanagawa 240-0005, Japan*

Seiji Taguma − *Tokyo Power Technology Ltd., Ohkuma, Fukushima 979-1305, Japan*

Katsushige Fujimoto − *Faculty of Symbiotic Systems Science, Cluster of Science and Technology, Fukushima University, Fukushima 960-1296, Japan*

Hikaru Sato − *Faculty of Symbiotic Systems Science, Cluster of Science and Technology, Fukushima University, Fukushima 960-1296, Japan;* Present Address: Faculty of Life and Environmental Sciences, University of Tsukuba, Ibaraki 305-8572, Japan

Naoaki Shibasaki − *Faculty of Symbiotic Systems Science, Cluster of Science and Technology, Fukushima University, Fukushima 960-1296, Japan; Institute of Environmental Radioactivity, Fukushima University, Fukushima 960-1296, Japan;* orcid.org/0000-0001-5213-2994

Complete contact information is available at: https://pubs.acs.org/10.1021/acsestwater.2c00455

Author Contributions

T.T.: Method setup, investigation, and writing paper draft. M.F.: ICP-MS analysis, investigation of PCA, and discussion. S.T: analysis of radioactivity concentration in Fukushima NPP. K.F: discussion and analysis of PCA analysis. H.S and N.S: discussion and drawing in local geology. Y.T.: conceptualization, supervision, and project administration. CRediT: **Tamao Tanji** formal analysis (lead), investigation (equal), methodology (equal), writing-original draft (lead); **Makoto Furukawa** formal analysis (equal), investigation (equal), methodology (equal); **Seiji Taguma** formal analysis (equal); **Katsushige Fujimoto** data curation (equal), validation (equal); **Hikaru Sato** data curation (equal), software (equal); **Naoaki Shibasaki** data curation (equal), investigation (equal), software (equal); **Yoshitaka Takagai** conceptualization (lead), data curation (equal), funding acquisition (lead), investigation (equal), methodology (lead), project administration (lead), supervision (lead), validation (lead), writing-original draft (equal), writing-review & editing (lead).

Notes

The authors declare no competing financial interest.

■ ACKNOWLEDGMENTS

The authors gratefully acknowledge funding by the JAEA Nuclear Energy S&T and Human Resource Development Project through concentrating wisdom Grant Number JPJA19H19210081 and the Japan Society for the Promotion of Science (JSPS) Grant-in-Aid for Scientific Research (B) 20H04352.

■ REFERENCES

(1) Querfeld, R.; Pasi, A. E.; Shozugawa, K.; Vockenhuber, C.; Synal, H. A.; Steier, P.; Steinhauser, G. Radionuclides in Surface Waters around the Damaged Fukushima Daiichi NPP One Month after the Accident: Evidence of Significant Tritium Release into the Environment. *Sci. Total Environ.* **2019**, *689*, 451−456.

(2) Tokyo Electric Power Company Holdings Inc.. Results of Radioactive Material Analysis in the Vicinity of the Fukushima Daiichi Nuclear Power Station. https://www.tepco.co.jp/en/hd/decommission/data/analysis/index-e.html.

(3) Shibasaki, N. Contaminated Water Issues at Fukushima Daiichi Nuclear Power Station: Its Geological Background and Challenges (Earth Scientific Challenge of Nuclear Power Station). *Earth Sci. (Chikyu Kagaku)* **2015**, *69*, 267−282.

(4) Castrillejo, M.; Casacuberta, N.; Breier, C. F.; Pike, S. M.; Masqué, P.; Buesseler, K. O. Reassessment of ^{90}Sr, ^{137}Cs, and ^{134}Cs in the Coast off Japan Derived from the Fukushima Dai-Ichi Nuclear Accident. *Environ. Sci. Technol.* **2016**, *50*, 173−180.

(5) Harkness, J. S.; Darrah, T. H.; Moore, M. T.; Whyte, C. J.; Mathewson, P. D.; Cook, T.; Vengosh, A. Naturally Occurring versus Anthropogenic Sources of Elevated Molybdenum in Groundwater: Evidence for Geogenic Contamination from Southeast Wisconsin, United States. *Environ. Sci. Technol.* **2017**, *51*, 12190−12199.

(6) McArthur, J. M.; Nath, B.; Banerjee, D. M.; Purohit, R.; Grassineau, N. Palaeosol Control on Groundwater Flow and Pollutant Distribution: The Example of Arsenic. *Environ. Sci. Technol.* **2011**, *45*, 1376−1383.

(7) Zhang, G.; Lu, P.; Wei, X.; Zhu, C. Impacts of Mineral Reaction Kinetics and Regional Groundwater Flow on Long-Term CO_2 Fate at Sleipner. *Energy Fuels* **2016**, *30*, 4159−4180.

(8) An, T. D.; Tsujimura, M.; Phu, V. L.; Kawachi, A.; Ha, D. T. Chemical Characteristics of Surface Water and Groundwater in Coastal Watershed, Mekong Delta, Vietnam. *Procedia Environ. Sci.* **2014**, *20*, 712−721.

(9) Bro, R.; Smilde, A. K. Principal Component Analysis. *Anal. Methods* **2014**, *6*, 2812−2831.

(10) Amirvaresi, A.; Parastar, H. External Parameter Orthogonalization-Support Vector Machine for Processing of Attenuated Total Reflectance-Mid-Infrared Spectra: A Solution for Saffron Authenticity Problem. *Anal. Chim. Acta* **2021**, *1154*, No. 338308.
(11) Kiss, J.; Sass-Kiss, A. Protection of Originality of Tokaji Aszú: Amines and Organic Acids in Botrytized Wines by High-Performance Liquid Chromatography. *J. Agric. Food Chem.* **2005**, *53*, 10042−10050.
(12) Jumhawan, U.; Putri, S. P.; Yusianto; Marwani, E.; Bamba, T.; Fukusaki, E. Selection of Discriminant Markers for Authentication of Asian Palm Civet Coffee (Kopi Luwak): A Metabolomics Approach. *J. Agric. Food Chem.* **2013**, *61*, 7994−8001.
(13) L'Annunziata, M.*Handbook of Radioactivity Analysis*, 3rd ed.; Academic Press, 2012.
(14) Yamada, N. Kinetic Energy Discrimination in Collision/Reaction Cell ICP-MS: Theoretical Review of Principles and Limitations. *Spectrochim. Acta, Part B* **2015**, *110*, 31−44.
(15) Secretariat of the Team for Countermeasures for Decommissioning and Contaminated Water Treatment. Summary of Decommissioning and Contaminated Water Management. https://www.meti.go.jp/english/earthquake/nuclear/decommissioning/pdf/20180329_e.pdf.
(16) Hirayama, H. Studies on Total Beta Measurements at Fukushima Daiichi Nuclear Power Station of Tokyo Electric Power Company with Egs5. *Jpn. J. Health Phys.* **2018**, *53*, 294−301.
(17) Lehto, J.; Xiaolin, H.Determination of Chemical Yield in Radiostrontium Separtion. In *Chemistry and Analysis of Radionuclides: Laboratory Techniques and Methodology*; Wiley-VCH Verlag GmbH & Co. KGaA, 2011; p 110.
(18) Tokyo Electric Power Company Holdings Inc.Efforts to ensure ocean protection -Subdrain operations and Seaside impermeable wall closing. https://www.tepco.co.jp/en/nu/fukushima-np/handouts/2015/images/handouts_150902_01-e.pdf.
(19) Liang, Z.; Chen, J.; Jiang, T.; Li, K.; Gao, L.; Wang, Z.; Li, S.; Xie, Z. Identification of the Dominant Hydrogeochemical Processes and Characterization of Potential Contaminants in Groundwater in Qingyuan, China, by Multivariate Statistical Analysis. *RSC Adv.* **2018**, *8*, 33243−33255.
(20) Yang, J.-J.; Liu, C.-C.; Chen, W.-H.; Yuan, C.-S.; Lin, C. Assessing the Altitude Effect on Distributions of Volatile Organic Compounds from Different Sources by Principal Component Analysis. *Environ. Sci.: Processes Impacts* **2013**, *15*, No. 972.
(21) Gonçalves, C. M.; Da Silva, J. C. G. E.; Alpendurada, M. F. Evaluation of the Pesticide Contamination of Groundwater Sampled over Two Years from a Vulnerable Zone in Portugal. *J. Agric. Food Chem.* **2007**, *55*, 6227−6235.
(22) Sakuma, K.; Kitamura, A.; Malins, A.; Kurikami, H.; Machida, M.; Mori, K.; Tada, K.; Kobayashi, T.; Tawara, Y.; Tosaka, H. Characteristics of Radio-Cesium Transport and Discharge between Different Basins near to the Fukushima Dai-Ichi Nuclear Power Plant after Heavy Rainfall Events. *J. Environ. Radioact.* **2017**, *169*−*170*, 137−150.
(23) Ansari, M. A.; Mohokar, H. V.; Deodhar, A.; Jacob, N.; Sinha, U. K. Distribution of Environmental Tritium in Rivers, Groundwater, Mine Water and Precipitation in Goa, India. *J. Environ. Radioact.* **2018**, *189*, 120−126.
(24) Zheng, Y.; He, W.; Li, B.; Hur, J.; Guo, H.; Li, X. Refractory Humic-like Substances: Tracking Environmental Impacts of Anthropogenic Groundwater Recharge. *Environ. Sci. Technol.* **2020**, *54*, 15778−15788.
(25) Moore, M. F.; Vasconcelos, J. G.; Zech, W. C.; Soares, E. P. A Procedure for Resolving Thermal Artifacts in Pressure Transducers. *Flow Meas. Instrum.* **2016**, *52*, 219−226.
(26) Engelhardt, I.; Prommer, H.; Schulz, M.; Vanderborght, J.; Schüth, C.; Ternes, T. A. Reactive Transport of Iomeprol during Stream-Groundwater Interactions. *Environ. Sci. Technol.* **2014**, *48*, 199−207.
(27) Tokyo Electric Power Company Holdings Inc.Status of Contaminated Water Measures.. https://www.tepco.co.jp/en/hd/decommission/progress/watermanagement/index-e.html.
(28) Tokyo Electric Power Company Holdings Inc.Completion of Seaside Impermeable Wall Closure at Fukushima Daiichi Nuclear Power Station. https://www.tepco.co.jp/en/nu/fukushima-np/handouts/2015/images/handouts_151026_01-e.pdf.
(29) Elliotis, M. C. A Mathematical Model for a Steady-State Seepage Flow of Groundwater under a Reinforced Concrete Dam. *Appl. Comput. Geosci.* **2019**, *1*, No. 100003.
(30) Sato, H.; Shibasaki, N.Chapter 6: Groundwater Flow at FDNPS. In *Geological and Hydrogeological Issues of Fukushima Daiichi Nuclear Power Station: Current Conditions and Challenges of 10 Years after the Nuclear Accident*; The Association for the Geological Collaboration in Japan: Tokyo, 2021; pp 127−154.
(31) Tokyo Electric Power Company Holdings Inc.. Radioactive Concentration measured by Seawater Radiation Monitor near Fukushima Daiichi Nuclear Power Station. https://www.tepco.co.jp/en/hd/decommission/data/monitoring/seawater/index-e.html.

https://doi.org/10.1021/acsestwater.2c00455
ACS EST Water 2023, 3, 139−146